

1
2 **Photodegradation of polycyclic aromatic hydrocarbons in**
3 **soils under a climate change base scenario**
4
5

6 Montse Marquès ^{a,b}, Montse Mari ^{a,b}, Carme Audí-Miró ^c, Jordi Sierra ^{b,d},
7 Albert Soler ^c, Martí Nadal ^{a,*}, José L. Domingo ^a
8
9

10 ^a *Laboratory of Toxicology and Environmental Health, School of Medicine, IISPV, Universitat*
11 *Rovira i Virgili, Sant Llorenç 21, 43201 Reus, Catalonia, Spain*

12 ^b *Environmental Engineering Laboratory, Departament d'Enginyeria Química, Universitat*
13 *Rovira i Virgili, Av. Països Catalans 26, 43007 Tarragona, Catalonia, Spain*

14 ^c *Grup de Mineralogia Aplicada i Geoquímica de Fluids, Departament de Cristal·lografia,*
15 *Mineralogia i Dipòsits Minerals, Facultat de Geologia, SIMGEO UB-CSIC, Universitat de*
16 *Barcelona UB, Martí Franquès s/n, 08028 Barcelona, Spain*

17 ^d *Laboratory of Soil Science, Faculty of Pharmacy, Universitat de Barcelona, Av. Joan XXIII*
18 *s/n, 08028 Barcelona, Catalonia, Spain*
19
20
21
22
23
24
25

26 -----
27 * Corresponding author. Tel.: +34 977 758930; fax: +34 977 759322.
28 *E-mail address: marti.nadal@urv.cat (M. Nadal).*
29

30 ABSTRACT

31

32 The photodegradation of polycyclic aromatic hydrocarbons (PAHs) in two typical
33 Mediterranean soils, either coarse- or fine-textured, was here investigated. Soil samples,
34 spiked with the 16 USEPA priority PAHs, were incubated in a climate chamber at stable
35 conditions of temperature (20°C) and light (9.6 W m⁻²) for 28 days, simulating a climate
36 change base scenario. PAH concentrations in soils were analyzed throughout the
37 experiment, and correlated with data obtained by means of Microtox[®] ecotoxicity test.
38 Photodegradation was found to be dependent on exposure time, molecular weight of each
39 hydrocarbon, and soil texture. Fine-textured soil was able to enhance sorption, being
40 PAHs more photodegraded than in coarse-textured soil. According to the EC₅₀ values
41 reported by Microtox[®], a higher detoxification was observed in fine-textured soil, being
42 correlated with the outcomes of the analytical study. Significant photodegradation rates
43 were detected for a number of PAHs, namely phenanthrene, anthracene, benzo(*a*)pyrene,
44 and indeno(*123-cd*)pyrene. Benzo(*a*)pyrene, commonly used as an indicator for PAH
45 pollution, was completely removed after 7 days of light exposure. In addition to the PAH
46 chemical analysis and the ecotoxicity tests, a hydrogen isotope analysis of
47 benzo(*a*)pyrene was also carried out. The degradation of this specific compound was
48 associated to a high enrichment in ²H, obtaining a maximum δ²H isotopic shift of +232‰.
49 This strong isotopic effect observed in benzo(*a*)pyrene suggests that compound-specific
50 isotope analysis (CSIA) may be a powerful tool to monitor *in situ* degradation of PAHs.
51 Moreover, hydrogen isotopes of benzo(*a*)pyrene evidenced a degradation process of
52 unknown origin occurring in the darkness.

53

54

55 *Keywords:*

56 Polycyclic aromatic hydrocarbons (PAHs)

57 Photodegradation

58 Soil

59 Ecotoxicity

60 Hydrogen isotopes

61 1. Introduction

62

63 Polycyclic aromatic hydrocarbons (PAHs) are a large group of semi-volatile organic
64 compounds composed of two or more fused aromatic rings. Although these chemicals are
65 mostly released to air, soil is considered as one of the major sinks of atmospheric PAHs
66 (Nadal et al., 2011; Wang et al., 2014), being deposited via dry and wet processes (Nadal
67 et al., 2004). PAH fate in the environment includes volatilization, adsorption on soil
68 particles, leaching, microbial degradation, chemical oxidation, and photo-oxidation
69 (Hartiash and Kaushik, 2009). Photodegradation is an important transformation pathway
70 for most PAHs in the environment (Zhang et al., 2006), having been largely studied in
71 water (Bertilsson and Widenfalk, 2002; de Bruyn et al., 2012; Fasnacht and Blough, 2003;
72 García-Martínez et al., 2005; Jacobs et al., 2008; Jing et al., 2014; Luo et al., 2014; Rivas
73 et al., 2000; Shemer and Linden, 2007; Singh et al., 2013; Xia et al., 2009). In contrast,
74 the knowledge regarding the photodegradation process of PAHs in soils is rather limited
75 (Balmer et al., 2000; Frank et al., 2002; Gong et al., 2001; Xiaozhen et al., 2005). It has
76 been reported that soil depth has an important role in the photodegradation of these
77 chemicals, enhancing the resistance of PAHs to be photodegraded. In addition,
78 temperature, soil particle size and humic acids also have a significant influence on
79 photodegradation in soils under UV-B radiation (Zhang et al., 2010). Photodegradation
80 of PAHs in soils has been shown to be not only limited by the light penetration capacity
81 in soils, but also by its wavelength (Cavoski et al., 2007; Xiaozhen et al., 2005).
82 Consequently, photodegradation depends on a number of variables, such as soil type,
83 thickness of the soil layer, as well as light absorption spectrum of each compound (Zhang
84 et al., 2010). This degradation process may play a key role on the fate of PAHs in areas
85 such as the Mediterranean region, with high sunlight presence during the whole year. In
86 turn, some PAH metabolites, which can even be more toxic than their parental
87 compounds, may be generated during the degradation process. Overall, although PAH
88 levels might be reduced in soils exposed to sunlight, toxicity may be increased (Huang et
89 al., 1995; Mallakin et al., 1999; McConkey et al., 1997).

90 Compound-specific isotope analysis (CSIA) is a very valuable tool, which can be used
91 to monitor *in situ* degradation processes of chemical pollutants, and as a source
92 identification technique (Elsayed et al., 2014; Imfeld et al., 2014). CSIA is capable of
93 discriminating degradation from other attenuation processes naturally occurring in the
94 environment, that do not generate destruction of pollutants, such as dispersion,

95 volatilization or sorption. CSIA is based on the isotopic effect produced during a
96 degradation process, which is known as isotopic fractionation (Meckenstock et al., 2004).
97 This effect is based on the enrichment of heavy isotopes in the reacting compound, which
98 is linked to the different strength of the bonds that contain heavy and light isotopes. Since
99 nondestructive natural attenuation processes frequently do not entail significant isotope
100 fractionation, a significant enrichment of the heavy isotope of organic pollutants confirms
101 that a degradation process is occurring. Unfortunately, research on the hydrogen isotopic
102 fractionation of PAHs during degradation is very scarce. To the best of our knowledge,
103 the only precedent is the study of Bergmann et al. (2011), who reported a high hydrogen
104 isotopic shift of naphthalene in two different microbial cultures.

105 The present investigation aimed at assessing the photodegradation of 16 US EPA
106 priority PAHs in two types of Mediterranean soils. Laboratory experiments were
107 conducted in a climate chamber to simulate the current Mediterranean environmental
108 conditions, keeping temperature and sunlight stable. Temporal changes of PAH
109 concentrations and ecotoxicity levels were investigated, and jointly evaluated. Moreover,
110 hydrogen isotopic analysis of benzo(*a*)pyrene, considered one of the most toxic PAHs
111 and probably carcinogenic to humans (Aina et al., 2006), was complementarily performed
112 to verify the findings.

113

114 **2. Materials and methods**

115

116 *2.1. Soil characteristics*

117

118 Two common Mediterranean soils were selected to perform the photodegradation
119 experiments. Physicochemical properties of both soils are given in Table 1. Soil samples
120 were collected from the A horizon of remote areas of Catalonia (NE of Spain). The
121 Arenosol soil, with granitic origin, is an acidic and coarse-textured soil that can be
122 classified as Haplic Arenosol, according to the (FAO-UNESCO, 1998). It is commonly
123 used for ecotoxicity tests in terrestrial environments. In turn, Regosol soil is an alkaline
124 calcareous fine-textured soil formed of sedimentary materials, being classified as Calcaric
125 Regosol (FAO-UNESCO, 1998). Both soils are characterized by owing a low organic
126 matter content (Table 1). In order to quantify titanium, iron, aluminum and manganese
127 oxides, ammonium oxalate was used as extractant, according to the method described by
128 Drees and Ulery (2008).

129

130 2.2. *Experimental design*

131

132 Photodegradation experiments were carried out in a Binder KBWF 240 climate
133 chamber (Binder GmbH, Tuttlingen, Germany) with constant lighting, temperature and
134 humidity. Temperature and daylight were set at 20 °C and 9.6 W/m², respectively, as
135 current environmental conditions in the Mediterranean area. Because photodegradation
136 reactions occur mainly in the surface, soil was air-dried. Consequently, to avoid the
137 presence of water and any potentially associated biodegradation process, humidity was
138 kept constant at 40%. Ten grams of air-dried soil were deployed in uncovered glass Petri
139 dishes forming a thick layer of 1 mm of soil. A stock solution containing 16 US EPA
140 priority PAHs at 2000 µg mL⁻¹ in dichloromethane:benzene was provided by Supelco®
141 (99.0% purity, Bellefonte, PA, USA). Each sample was 10-times spiked with 25 µL of
142 this stock solution diluted with an hexane/dichloromethane (1:1) mixture (Scharlau
143 Chemie S.A., Barcelona, Spain; hexane: 96% purity, dichloromethane: 99.5% of purity)
144 to an individual PAH concentration of 100 µg mL⁻¹, leading to a Σ16 PAHs concentration
145 of 40 µg g⁻¹ in soil. Afterwards, samples were incubated inside the climate chamber. In
146 order to differentiate concentration decreases due to slow sorption and/or volatilization
147 processes from photodegradation, a number of dark control samples covered with
148 aluminum foil were exposed to the same environmental conditions. Duplicates of
149 irradiated samples and dark controls of each soil were removed from the climate chamber
150 after 1, 2, 3, 4, 5, 6, 7, 14, and 28 days. To verify the lack of any biotic reactions, before
151 the experiment was initiated, soils were incubated at the same conditions in manometric
152 respirometers (Oxitop®, WTW). Negligible oxygen consumption was observed during the
153 incubation period, discarding biotic processes. Ten grams of soil without any spiking of
154 PAHs were used as blank soil samples.

155

156 2.3. *PAH analysis*

157

158 Prior to analysis, PAHs were extracted from soil samples by using 30 mL of a mixture of
159 hexane/dichloromethane (1:1) (Scharlau Chemie S.A., Barcelona) in a Milestone Start E
160 Microwave Extraction System (Milestone s.r.l., Sorisole, Italy), according to the US EPA
161 method 3546. Subsequently, samples were filtered, concentrated to 1 mL and further
162 evaporated with a gentle stream of purified N₂. Since any interference with target analytes

163 was found, cleanup was discarded in order to achieve suitable recoveries for low
164 molecular weight PAHs. Regarding the quality control, d₁₀-fluorene (98.3% purity,
165 Supelco[®]) was used as surrogate, while d₈-naphthalene (99.8% purity, Supelco[®]) and d₁₂-
166 benzo(a)pyrene (98.5% purity, Supelco[®]) were used as internal standards. Dried samples
167 were dissolved with a solution of internal standards at 50 µg mL⁻¹ concentration in
168 hexane/dichloromethane (1:1) mixture (Scharlau Chemie S.A., 99.5% of purity). Blank
169 soil samples were also extracted following the same procedure in order to assure that
170 collected soils were PAH-free. All samples were analyzed by means of gas
171 chromatography-mass spectrometry (GC-MS) in accordance to the US EPA method
172 8270. A Hewlett-Packard G1099A/MSD5973 equipment with an HP-5MS 5% Phenyl
173 Methyl Siloxane column (20 m x 0.25 mm x 0.25 µm) was used to quantify the content
174 of the 16 PAHs under study in soil. The final experimental conditions were: 1 µL injection
175 at 310 °C in split-splitless, and pulsed splitless mode at 35 psi (for 0.05 min). Transfer
176 line temperature was set at 280 °C. Ultra-pure (99.9999%) helium was used as carrier gas,
177 at a total flow rate of 1.4 mL min⁻¹. The GC oven temperature started at 80 °C, being
178 consecutively increased at 15 °C min⁻¹ until 180 °C, at 8 °C min⁻¹ until 250 °C, and at 3
179 °C min⁻¹ up to 300 °C. At the end of each ramp, temperature was held for 1 min. Finally,
180 an increase of 20 °C min⁻¹ was executed until reaching 320 °C, holding this temperature
181 for 6 min. The detector was set to quantify the analytes covering specific masses ranging
182 from 40 to 600 atomic mass units. The mass spectrometer and source temperatures were
183 150 °C and 230 °C, respectively. Samples were quantified using a six-point calibration
184 curve (5, 10, 25, 50, 60, 80 µg mL⁻¹). Sample preparation for the PAH analyses was
185 performed at the “Laboratory of Environmental Engineering” of THE Universitat Rovira
186 i Virgili (URV), while concentrations were determined at the “Servei de Recursos
187 Científics i Tècnics” of the same institution (SRCiT-URV).

188

189 *2.4. Statistical analysis*

190

191 Results were statistically evaluated using XLSTAT Statistical Software for Excel.
192 Repeated measures of the ANOVA were used to state significant differences between
193 irradiated and non-irradiated samples through the time. A regression analysis was also
194 executed to study the relationship between concentrations and time. Probability levels
195 were considered as statistically significant at p<0.05.

196

197 2.5. *Ecotoxicological tests*

198

199 Soils were extracted by using an ultrasonic bath mixture (1:1) of n-hexane 95% (UV-
200 IR-HPLC) PAI-ACS (Panreac, Castellar del Vallès, Barcelona, Spain) and acetone (Reag.
201 Ph. Eur) PA-ACS-ISO (Panreac), following the US EPA method 3550C. Blank soil
202 samples were simultaneously extracted following the same procedure. Afterwards, soil
203 extracts were filtered, and the solvent was completely dried with a rotatory evaporator,
204 being finally reconstituted with 2 mL of dimethyl sulfoxide (UV-IR-HPLC-GPC) to a
205 concentration of 2-4% in Microtox diluent (2% NaCl of aqueous solution). Ecotoxicity
206 values were quantified by means of the Microtox[®] 500 Analyser (SDI, USA), following
207 the ISO 11348-1:2007 norm. The bioluminescent bacteria *V. fischeri* was used to measure
208 the inhibition of light emission when organisms were exposed to soil extract samples.
209 EC₅₀ values were estimated as the sample concentration causing 50% of light inhibition
210 on the test organisms (Roig et al., 2013). Sample preparation and Microtox[®] test were
211 performed at the “Laboratory of Environmental Engineering” of the URV.

212

213 2.6. *Hydrogen isotope analysis of benzo(a)pyrene*

214

215 For hydrogen isotope analysis, soil samples were also extracted with the same
216 Milestone Start E Microwave Extraction System (Milestone s.r.l., Sorisole, Italy),
217 according to the US EPA method 3546. The extract was treated by following the same
218 procedure used to analyze PAH levels. Once the extract was completely dried, it was
219 dissolved in 62.5 µL of dichloromethane (99.5%, Scharlau Chemie S.A.) free of any
220 deuterated PAHs that could interfere in δ²H analysis. The hydrogen isotope composition
221 of benzo(a)pyrene was analyzed using a gas chromatography-pyrolysis-isotope ratio
222 mass spectrometry system (GC-Pyr-IRMS) consisting of a Trace GC Ultra equipped with
223 a split/splitless injector, coupled to a Delta V Advantage IRMS (Thermo Scientific
224 GmbH, Bremen, Germany), through a combustion interface.

225 The GC/Pyr/IRMS system was equipped with an Agilent Technologies DB-1 column
226 (30 m × 0.25 mm, 1.0 µm film thickness; Santa Clara, CA, USA). The oven temperature
227 program was kept at 50 °C for 1 min, heated again until 160 °C at a rate of 25 °C min⁻¹,
228 then up to 320 °C at a rate of 3 °C min⁻¹, being finally held at 320 °C for 20 min. The
229 injector was set to splitless mode at a temperature of 280 °C. Helium was used as a carrier
230 gas with a gas flow rate of 1.0 mL min⁻¹.

231 Hydrogen isotope ratios are reported relative to an international standard (Vienna
232 Standard Mean Ocean Water, VSMOW), using the delta notation:

$$233 \quad \delta^2\text{H} (\text{‰}) = (R/R_{\text{std}} - 1) \times 1000$$

234 where R and R_{std} are the isotope ratios (H^2/H^1) of the sample and the standard,
235 respectively. All the measurements were run in duplicate, and the standard deviations of
236 the $\delta^2\text{H}$ values obtained were below $\pm 10\text{‰}$. The analytical system was daily verified using
237 PAH control standards with known hydrogen isotope ratios, which were previously
238 determined using a Carlo-Erba 1108 (Carlo-Erba, Milano, Italy) elemental analyzer (EA)
239 coupled in continuous flow to a Delta Plus XP isotope ratio mass spectrometer (Thermo
240 Fisher Scientific, Bremen, Germany). The samples were prepared for the isotopic
241 analyses in the “Mineralogia Aplicada i Geoquímica de Fluids” Research Group
242 laboratory and analyzed at the “Centres Científics i Tecnològics” of the Universitat de
243 Barcelona (CCiT-UB).

244

245 **3. Results and discussion**

246

247 *3.1. Photodegradation of PAHs in soils*

248

249 The trends in the levels of naphthalene, phenanthrene, pyrene, benzo(a)pyrene, and
250 benzo(g,h,i)perylene in Arenosol and Regosol soils, are depicted in Fig. 1. Those
251 compounds were selected as representatives of 2-, 3-, 4-, 5- and 6-ringed PAHs,
252 respectively. The results for other PAHs are shown in Supporting Information (SI, Fig.
253 S1). A different behavior for the 16 PAHs in coarse- and fine-textured soils over the time
254 was observed, leading to different photodegradation rates, which were calculated
255 considering the difference between irradiated samples and dark controls (Table 2).
256 Statistical significances for the different exponential and linear rates are shown in Table
257 3. Three main processes might be related to the concentration decreases: volatilization
258 (Wang et al., 2015), sorption (Liu et al., 2007; Zhang et al., 2014), and photodegradation
259 (EL-Saeid et al., 2015). However, the contribution of each process was different
260 according to the physicochemical properties of each compound (SI, Table S1), as well as
261 to the texture of each soil. In general terms, higher photodegradation rates were noted in
262 some compounds for fine-textured soil, when comparing irradiated samples and dark
263 controls. As expected, the lowest PAH recoveries were found for the most volatile
264 compounds (naphthalene, acenaphthylene and acenaphthene). PAH recoveries 1 h after

265 soil contamination were found to be higher in fine-textured Regosol soil (14%-127%)
266 than in heterogeneous coarse-textured Arenosol soil (7%-92%). The latter has lower
267 organic matter content, as well as a lower amount of fine fraction, causing a weaker
268 retention of PAHs.

269 Volatilization was probably the most significant process for 2- and 3-ringed PAHs. No
270 differences of naphthalene concentrations were found between irradiated and dark control
271 samples, indicating that naphthalene was not photodegraded in any soil, either Arenosol
272 or Regosol. Because of its high vapor pressure, the decreasing content of naphthalene
273 (85%) observed during the first hour after being spiked (SI, Table S1) could be related to
274 volatilization processes (Liu et al., 2011). Similar results were also obtained for
275 acenaphthylene, being 80% decreased in the same period of time elapsed. Regarding
276 acenaphthene, similar and constant concentrations were noted for irradiated and dark
277 control samples over the time, with slight decreasing rates in Arenosol and Regosol soils
278 (1.5% and 2%, respectively). Consequently, a significant decrease of the concentration of
279 this compound was not observed ($p>0.05$), indicating that photodegradation did not occur.

280 Fluorene, phenanthrene, anthracene and fluoranthene showed higher decreasing
281 concentration rates in Regosol than in Arenosol soil. In Regosol soil, phenanthrene and
282 anthracene exhibited photodegradation rates of 33% and 40%, respectively, after 28 days
283 of light exposure, being the differences between controls and irradiated samples
284 statistically significant after 2 days.

285 In Arenosol soil, pyrene, benzo(*a*)anthracene, chrysene and benzo(*b+k*)fluoranthene
286 kept their concentrations constant in both irradiated samples and dark controls, suggesting
287 lack of photodegradation. In contrast, decreasing concentrations of the same 4-ringed
288 PAHs were found in fine-textured Regosol soil. Decreasing rates were up to 30% for these
289 compounds at the end of the experiment. In turn, pyrene concentration was only slightly
290 decreased (17%) over the experiment. This ratio is 10% lower than that reported by
291 (Zhang et al., 2010) for pyrene in soil samples irradiated using UV lamps with a
292 wavelength of 254 nm. However, no significant differences were noted in the current
293 study between irradiated and control samples ($p>0.05$).

294 Benzo(*a*)pyrene was sorbed to soil during the first day according to the fast
295 concentration decrease, in both soils and both irradiated and non-irradiated samples. A
296 decreased rate of 23% was estimated in coarse-textured Arenosol soil, which is in
297 agreement with the findings of Zhang et al. (2006). In turn, higher rates were observed in
298 fine-textured Regosol soil, showing a complete removal of benzo(*a*)pyrene after 7 days

299 of incubation. Zhang et al. (2008) reported that titanium dioxide (TiO₂) under UV light,
300 accelerates the photodegradation process of phenanthrene, pyrene and benzo(*a*)pyrene on
301 surface soil, being benzo(*a*)pyrene the most quickly degraded. Although the TiO₂ content
302 in fine-textured Regosol soil is lower than that in Arenosol soil, the higher content of
303 other photocatalysts (e.g., Fe₂O₃, Al₂O₃, MnO₂, or TiO₂) in the fine-textured soil, as well
304 as the higher fine fraction due to its clay content, might be responsible of this complete
305 degradation (Gupta and Gupta, 2015; Zhang et al., 2006; Zhao et al., 2004).

306 As a consequence of the high constant concentrations in irradiated samples and dark
307 controls, it can be confirmed that dibenzo(*a,h*)anthracene tended to be less adsorbed than
308 other PAHs in both soils, since concentrations in dark controls were constant over the
309 experiment. This compound seemed to suffer a slight photodegradation in the coarse-
310 textured soil, while the degradation rate was substantially higher in fine-textured soil
311 (<5% and 28%, respectively) over the experiment. After 28 days of exposure, only 12%
312 of the indeno(*123-cd*)pyrene was photodegraded in Arenosol soil, while up to 69% was
313 removed in fine-textured Regosol soil. Benzo(*ghi*)perylene was adsorbed more quickly
314 in the coarsed soil, finding a slightly higher decrease of its concentration in dark controls
315 over the experiment when comparing to dibenzo(*a,h*)anthracene. The photodegradation
316 of benzo(*ghi*)perylene started in the 14th day of exposure, being the photodegradation rate
317 <5% after 28 days. Contrastingly, this PAH was less adsorbed in Regosol soil, where a
318 photodegradation of up to 25 % was noted at the end of the experiment.

319 Phenanthrene, pyrene, benzo(*a*)pyrene and benzo(*ghi*)perylene showed a concentration
320 decrease in dark conditions in Arenosol soil, indicating that unknown degradation
321 processes, other than photodegradation, could be also occurring in the dark conditions for
322 this type of soil. In contrast, in the Regosol soil, these same compounds showed constant
323 concentrations in dark conditions, being therefore different from the levels observed
324 under light conditions.

325 Focusing on the differences between soil textures, our findings agree with those
326 previously reported by Xiaozhen et al. (2005). These authors found that the photolysis
327 rate of antrazine and the photolytic depth increased gradually from sand through silt to
328 clay. Therefore, photochemical reactions may be accelerated when soil particles are
329 smaller. This is likely related to the increase of the surface area per mass, hence showing
330 a greater catalytic capability. By contrast, Zhang et al. (2010) found that the increase of
331 soil particle size allows a higher scattering and permeation of light, therefore speeding up
332 any photodegradation process. It must be stated that the current experiment was

333 performed with the top soil layer (1 mm of depth), since the objective was to analyze the
334 PAH photodegradation in soils due to atmospheric deposition. Consequently, in the
335 present study the role of light penetration is discarded. Several studies have also
336 highlighted the active function of Fe₂O₃, MnO and TiO₂ to boost photodegradation
337 processes. Zhao et al. (2004) found that the addition of α-Fe₂O₃ or TiO₂ enhanced the
338 photocatalytic degradation of gamma-hexachlorocyclohexane (γ-HCH) in the soil
339 surface. Similarly, Zhang et al. (2006) stated that the content of Fe₂O₃ and other
340 semiconductor oxides, such as TiO₂ and MnO₂, in soils improved the photodegradation
341 of benzo(a)pyrene. Notwithstanding, the presence of oxides available in fine-textured
342 Regosol soil, as well as its clay content, might have some influence on the high
343 photodegradation rates, even in the PAHs of high molecular weight. Nadal et al. (2006)
344 reported that high molecular weight PAHs could not be photodegraded in an organic
345 solvent after one week of UV-B exposure. In contrast, Guieysse et al. (2004) confirmed
346 found out that UV-photolysis acts preferentially on large PAHs. In any case, the
347 complexity of soils could give place to an enhancement and acceleration of
348 photodegradation reactions.

349

350 *3.2. Effect of photodegradation over ecotoxicity of PAHs*

351

352 Microtox[®] has been established as a fast, useful and sensitive method to assess the
353 toxicity of soils spiked with PAHs (Khan et al., 2012). According to Salizzato et al.
354 (1997), 5 min.-EC₅₀ values were found to be suitable for these organic compounds. In the
355 present study, blank samples in Arenosol and Regosol soils, showed ecotoxicity values
356 of 113 and 182 mg of soil mL⁻¹ Microtox[®] diluent, respectively. These results are 10-
357 times higher than toxicity results found in spiked soil samples before any irradiation,
358 showing values of 12.9 and 15.6 mg of soil mL⁻¹ Microtox[®] diluent, in Arenosol and
359 Regosol soil samples, respectively.

360 The EC₅₀ values of irradiated samples and dark controls in Arenosol and fine-textured
361 Regosol soils are depicted in Fig. 2. The coefficient of determination (R²) of EC₅₀ vs. Σ16
362 PAH concentrations over the time was 0.75 and 0.78 in coarse- and fine-textured soils,
363 respectively. Both irradiated samples and dark controls tended to increase their EC₅₀ over
364 time. This slow detoxification would be mainly consequence of the volatilization,
365 sorption and/or photodegradation of PAHs. In Arenosol samples, EC₅₀ of irradiated and
366 control samples showed a very similar trend. Therefore, no ecotoxicity differences were

367 found, independently on the exposure to light, being in full agreement with the findings
368 from the chemical analysis of PAHs. In contrast, EC₅₀ in irradiated and dark control
369 samples of fine-textured soils showed a different pattern (Fig. 2). Excluding data
370 regarding one day after incubation, the EC₅₀ curve of irradiated samples was more
371 pronounced than that of dark controls, indicating a lower toxicity. Taking into account
372 that irradiated and dark control samples were exposed to the same conditions, excepting
373 light exposure, it is clear that light enhances the detoxification of fine-textured Regosol
374 soil. Similarly to Arenosol soil findings, the current toxicity results also agree with the
375 high photodegradation rates observed in the analytical experiment. Those 3-, 4-, 5- and
376 6-ringed PAHs, which were highly photodegraded, could be the responsible of the
377 toxicity decrease. In the period of time elapsed between day 1 and before 2 and 3 days
378 after incubation time in Regosol and Arenosol soils, respectively, the toxicity of irradiated
379 samples was higher than in dark controls. This could be linked to the potential formation
380 of metabolites, such as some oxygenated PAHs, even more toxic than the parental
381 compounds (Bandowe et al., 2014; Knecht et al., 2013; Lundstedt et al., 2007). Anyhow,
382 this finding deserves further investigation, which should confirm the relationship between
383 the generation of by-products and the ecotoxicological status of soil.

384 The results of the Microtox[®] ecotoxicity test demonstrated that the light, together with
385 other mechanisms such as sorption, volatilization, and abiotic degradation, enhances PAH
386 detoxification on surface soil. This process is especially remarkable in fine-textured soils,
387 which contain materials capable to act as photocatalysts. Anyway, although
388 photodegradation and detoxification occurred, spiked soil samples did not achieve
389 toxicity levels of blank samples 28 days after light exposure. Consequently, a longer
390 exposure time, or an increase of light intensity, would be required to completely remove
391 PAHs from soils. However, the outcomes of both chemical and ecotoxicological analyses
392 indicate that photodegradation is an important process of PAH removal in soil.

393

394 *3.3. Hydrogen isotope effects on benzo(a)pyrene*

395

396 The hydrogen isotopic composition of benzo(a)pyrene in irradiated samples and dark
397 controls is shown in Fig. 3. In Arenosol soil, benzo(a)pyrene of irradiated samples
398 experienced a change in its hydrogen isotopic composition (after only 5 days of
399 experiment) from -39‰ to +193‰. In agreement with data on PAH levels, this high
400 isotopic shift clearly confirms degradation of benzo(a)pyrene under the selected climate

401 conditions. Due to their too low concentrations, $\delta^2\text{H}$ could not be obtained from the
402 subsequent samples. Unexpectedly, a hydrogen isotopic change of benzo(*a*)pyrene was
403 also observed in dark control samples. Therefore, unknown degradation processes could
404 be also occurring in absence of light (Fig. 3). Under darkness conditions, benzo(*a*)pyrene
405 in Arenosol suffered a progressive enrichment in $\delta^2\text{H}$. Despite being slower than in
406 irradiated samples, it increased from -39‰ to +181‰ after 28 days of incubation in the
407 dark. It is suggested that there could be some abiotic degradation of benzo(*a*)pyrene,
408 which would be the result of its reaction with organic and/or mineral phases of the soil.

409 The hydrogen isotope results of benzo(*a*)pyrene in Regosol soil samples were similar
410 to those corresponding to Arenosol soil. Benzo(*a*)pyrene hydrogen isotopic composition
411 changed from -39‰ to +68‰ after only 3 days of experiment (Fig. 3). Five days after
412 starting, a decrease in the $\delta^2\text{H}$ value was observed, most likely as a result of reversible
413 sorption processes, which might have released benzo(*a*)pyrene molecules with a lower
414 degradation degree, and consequently, with a lower $\delta^2\text{H}$. However, this isotopic shift also
415 confirms that benzo(*a*)pyrene in Regosol soil is degraded under the same climate
416 conditions. Dark controls also showed a slow degradation, with an isotopic change from
417 -39‰ to +35‰ after 28 days of experiment. Similarly to Arenosol soil samples, dark
418 controls of Regosol soil showed a slower isotopic enrichment in ^2H with respect to
419 irradiated samples, confirming that the same process of PAH loss might be occurring.
420 The evolution of the hydrogen isotopic composition of the dark controls shows
421 fluctuations over the time that could be linked to sorption/desorption effects.
422 Consequently, the hydrogen isotope analysis also seems to confirm that sorption
423 processes of PAHs in soil were present, which is in agreement with the data from the
424 chemical analysis of PAHs. Notwithstanding, since the relationship between the lack of
425 hydrogen isotopic fractionation of PAHs with sorption processes in soil has not been
426 described in the scientific literature, this hypothesis cannot be confirmed yet. Our results
427 corroborate that benzo(*a*)pyrene is not only photodegraded, but also that this degradation
428 is associated to a significant isotopic change. Moreover, they highlight the great potential
429 of CSIA to be used as a powerful tool to monitor *in situ* PAH degradation. Furthermore,
430 the abiotic degradation of benzo(*a*)pyrene without light intervention was proved to be a
431 potentially relevant pathway of PAH loss in soil. However, further studies are still
432 necessary to confirm the mechanisms of PAH degradation in dark conditions.

433

434 **4. Conclusions**

435

436 The photodegradation of PAHs in soils is highly dependent on the exposure time, the
437 molecular weight of each hydrocarbon, and the soil texture. Low molecular weight PAHs
438 are more influenced by volatilization and sorption, while medium and high molecular
439 weight PAHs are able to undergo different photodegradation ratios. Soil properties
440 (texture and metal oxides) were found to influence on volatilization, sorption and
441 photodegradation of PAHs. Photodegradation in soils is a mechanism that mostly occurs
442 in soil surface, being able to partially detoxify soil. Moreover, this process can be
443 enhanced by solid phase soil composition, especially in soils with a finer fraction, as well
444 as by the presence of semiconductor minerals, such as metal oxides. The evolution of 16
445 PAH concentrations over the time agrees well with Microtox[®] results, with a faster
446 detoxification in fine-textured Regosol soil. However, after 28 days of incubation, soil
447 samples were not completely detoxified. It is important to note that photodegradation is
448 not the only process of PAH loss in soils. Other mechanisms, such as biodegradation and
449 sorption, may also have important roles on the PAH behavior in soils. Moreover, in a
450 climate change context, where an increase of solar radiation is expected,
451 photodegradation could become a very important process in PAH dynamics in soils.

452 Finally, the complementary analyses of hydrogen isotopes of benzo(*a*)pyrene
453 confirmed, at a molecular level, that this compound is degraded not only under light
454 conditions, but also in the darkness. Furthermore, the strong isotopic effect observed in
455 benzo(*a*)pyrene makes the CSIA a potentially suitable technique to give evidence of PAH
456 degradation. Since its degradation involves a high hydrogen isotopic variation, CSIA is
457 also a powerful tool to quantify *in situ* the degradation efficiency.

458

459 **Acknowledgments**

460

461 This study was financially supported by the Spanish Ministry of Economy and
462 Competitiveness, through the projects CTM2012-33079 and CGL2011-29975-C04-01,
463 and by the Catalan Government, through the projects 2014SGR90 and 2014SGR1456.
464 Montse Marquès received a PhD fellowship from AGAUR (Commissioner for
465 Universities and Research of the Department of Innovation, Universities and Enterprise
466 of the “Generalitat de Catalunya” and the European Social Fund). The authors are
467 indebted to Josep Maria Mateo-Sanz for his excellent assistance in statistics analysis.

468

469 **References**

470

- 471 Aina, R., Palin, L., Citterio, S., 2006. Molecular evidence for benzo[a]pyrene and naphthalene
472 genotoxicity in *Trifolium repens* L. *Chemosphere* 65, 666-673.
- 473 Balmer, M.E., Goss, K.-U., Schwarzenback, R.P., 2000. Photolytic transformation of organic
474 pollutants on soil surfaces an experimental approach. *Environ. Sci. Technol.* 34, 1240-
475 1245.
- 476 Bandowe, B.A.M., Bigalke, M., Boamah, L., Nyarko, E., Saalia, F.K., Wilcke, W., 2014.
477 Polycyclic aromatic compounds (PAHs and oxygenated PAHs) and trace metals in fish
478 species from Ghana (West Africa): Bioaccumulation and health risk assessment. *Environ.*
479 *Int.* 65.
- 480 Bergmann, F.D., Abu Laban, N.M.F.H., Meyer, A.H., Elsner, M., Meckenstock, R.U., 2011. Dual
481 (C, H) isotope fractionation in anaerobic low molecular weight (Poly)aromatic
482 hydrocarbon (PAH) degradation: potential for field studies and mechanistic implications.
483 *Environ. Sci. Technol.* 45, 6947-6953.
- 484 Bertilsson, S., Widenfalk, A., 2002. Photochemical degradation of PAHs in freshwaters and their
485 impact on bacterial growth – influence of water chemistry. *Hydrobiologia.* 469, 23-32.
- 486 Cavoski, I., Caboni, P., Sarais, G., Cabras, P., Miano, T., 2007. Photodegradation of rotenone in
487 soils under environmental conditions. *J. Agric. Food Chem.* 55, 7069-7074.
- 488 de Bruyn, W.J., Clark, C.D., Ottelle, K., Aiona, P., 2012. Photochemical degradation of
489 phenanthrene as a function of natural water variables modeling freshwater to marine
490 environments. *Mar. Pollut. Bull.* 64, 532-538.
- 491 Drees, L.R., Ulery, A.L., 2008. *Methods of Soil Analysis. Part 5. Mineralogical Methods.* Soil
492 Science Society of America, 677 S. Segoe Road, Madisom, WI 53711, USA.
- 493 EL-Saeid, M.H., Al-Turki, A.M., Nadeem, M.E.A., Hassanin, A.S., Al-Wabel, M.I., 2015.
494 Photolysis degradation of polyaromatic hydrocarbons (PAHs) on surface sandy soil.
495 *Environ. Sci. Pollut. Res.* 22, 9603–9616.
- 496 Elsayed, O.F., Maillard, E., Vuilleumier, S., Nijenhuis, I., Richnow, H.H., Imfeld, G., 2014. Using
497 compound-specific isotope analysis to assess the degradation of chloroacetanilide
498 herbicides in lab-scale wetlands. *Chemosphere* 99, 89-95.
- 499 FAO-UNESCO, World Reference Base for Soil Resources. FAO, Rome, 1998.
- 500 Fasnacht, M.P., Blough, N.V., 2003. Mechanisms of the aqueous photodegradation of Polycyclic
501 Aromatic Hydrocarbons. *Environ. Sci. Technol.* 37, 5767-5772.
- 502 Frank, M.P., Graebing, P., Chib, J.S., 2002. Effect of soil moisture and sample depth on pesticide
503 photolysis. *J. Agric. Food Chem.* 50, 2607-2614.
- 504 García-Martínez, M.J., Canoira, L., Blazquez, G., Da Riva, I., Alcántara, R., Llamas, J.F., 2005.
505 Continuous photodegradation of naphthalene in water catalyzed by TiO₂ supported on
506 glass Raschig rings. *Chem. Eng. J.* 110, 123-128.
- 507 Gong, A., Ye, C., Wang, X., Lei, Z., Liu, J., 2001. Dynamics and mechanism of ultraviolet
508 photolysis of atrazine on soil surface. *Pest Manage. Sci.* 57, 380-385.
- 509 Guieysse, B., Viklund, G., Toes, A.C., Mattiasson, B., 2004. Combined UV-biological
510 degradation of PAHs. *Chemosphere* 55, 1493-1499.
- 511 Gupta, H., Gupta, B., 2015. Photocatalytic degradation of polycyclic aromatic hydrocarbon
512 benzo[a]pyrene by iron oxides and identification of degradation products. *Chemosphere*
513 138, 924–931.
- 514 Hartiash, A.K., Kaushik, C.P., 2009. Biodegradation aspects of Polycyclic Aromatic
515 Hydrocarbons (PAHs): A review. *J. Hazard. Mater.* 169, 1-15.
- 516 Huang, X., Dixon, D.G., Greenberg, B.M., 1995. Increased polycyclic aromatic hydrocarbon
517 toxicity following their photomodification in natural sunlight: Impacts on the duckweed
518 *Lemna gibba* L. G-3. *Ecotoxicol. Environ. Saf.* 32, 194-200.
- 519 Imfeld, G., Kopinke, F.D., Fischer, A., Richnow, H.H., 2014. Carbon and hydrogen isotope
520 fractionation of benzene and toluene during hydrophobic sorption in multistep batch
521 experiments. *Chemosphere* 107, 454-461.
- 522 Jacobs, L.E., Weavers, L.K., Chin, Y., 2008. Direct and indirect photolysis of polycyclic aromatic
523 hydrocarbons in nitrate-rich surface waters. *Environ. Toxicol. Chem.* 27, 1643-1648.

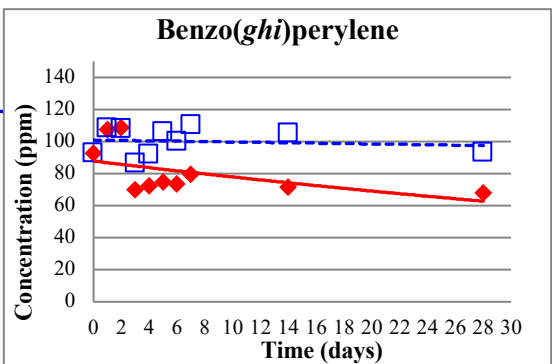
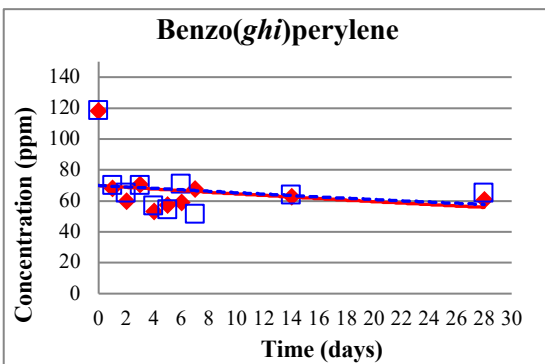
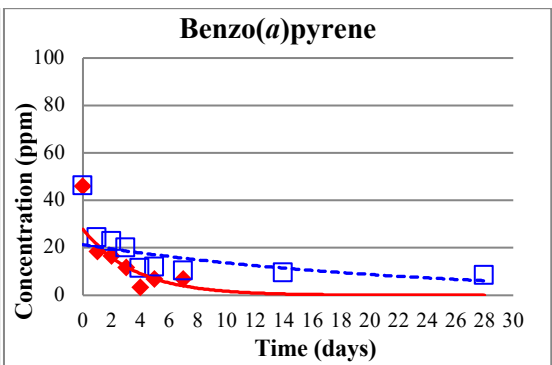
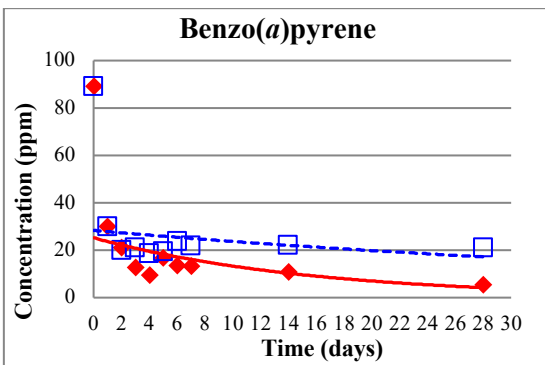
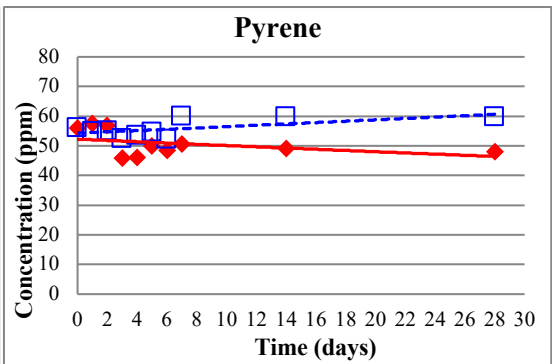
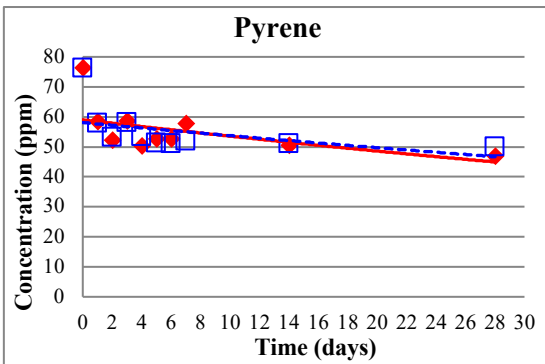
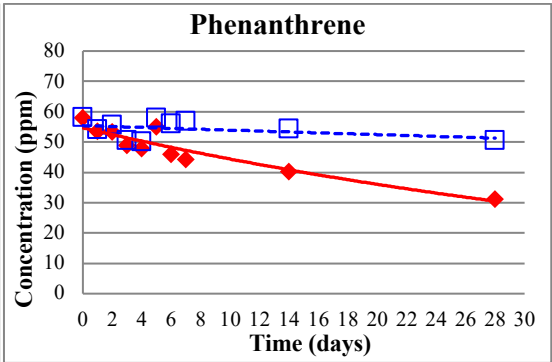
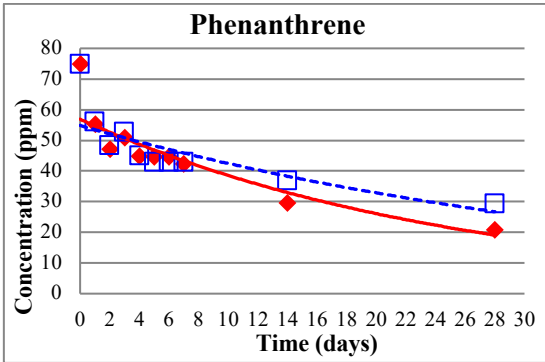
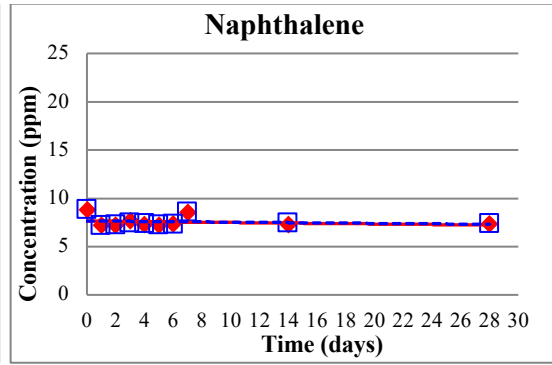
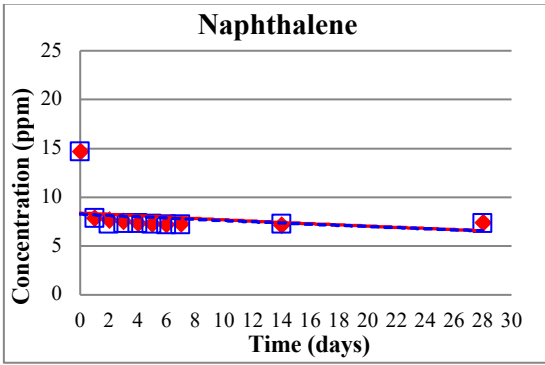
- 524 Jing, L., Chen, B., Zhang, B., Zheng, J., Liu, B., 2014. Naphthalene degradation in seawater by
525 UV irradiation: The effects of fluence rate, salinity, temperature and initial concentration.
526 Mar. Pollut. Bull. 81, 149-156.
- 527 Khan, M., Cheema, S.A., Tang, X., Shen, C., Sahi, S.T., Jabbar, A., Park, J., Chen, Y., 2012.
528 Biototoxicity assessment of pyrene in soil using a battery of biological assays. Arch.
529 Environ. Contam. Toxicol. 63, 503-512.
- 530 Knecht, A.L., Goodale, B.C., Truong, L., Simonich, M.T., Swanson, A.J., Matzke, M.M.,
531 Anderson, K.A., Waters, K.M., Tanguay, R.L., 2013. Comparative developmental
532 toxicity of environmentally relevant oxygenated PAHs. Toxicol. Appl. Pharmacol. 271,
533 266-275.
- 534 Liu, G., Yu, L., Li, J., Liu, X., Zhang, G., 2011. PAHs in soils and estimated air-soil exchange in
535 the Pearl River Delta, South China. Environ. Monit. Assess. 173, 861-870.
- 536 Liu, L., Tindall, J.A., Friedel, M.J., 2007. Biodegradation of PAHs and PCBs in soils and sludges.
537 Water Air Soil Pollut. 181, 281-296.
- 538 Lundstedt, S., White, P.A., Lemieux, C.L., Lynes, K.D., Lambert, I.B., Oberg, L., Haglund, P.,
539 Tysklind, M., 2007. Sources, fate, and toxic hazards of oxygenated polycyclic aromatic
540 hydrocarbons (PAHs) at PAH-contaminated sites. Ambio. 36, 475-485.
- 541 Luo, L., Wang, P., Lina, L., Luana, T., Keb, L., Fung Yee Tam, N., 2014. Removal and
542 transformation of high molecular weight polycyclic aromatic hydrocarbons in water by
543 live and dead microalgae. Process Biochem. 49, 1723-1732.
- 544 Mallakin, A., McConkey, B.J., Miao, G., McKibben, B., Snieckus, V., Dixon, D.G., Greenberg,
545 B.M., 1999. Impacts of structural photomodification on the toxicity of environmental
546 contaminants: anthracene photooxidation products. Ecotoxicol. Environ. Saf. 43, 204-
547 212.
- 548 McConkey, B.J., Duxbury, C.L., Dixon, D.G., Greenberg, B.M., 1997. Toxicity of PAH
549 photooxidation product to the bacteria *Photobacterium Phosphoreum* and the duckweed
550 *Lemna Gibba*: effects of phenanthrene and its primary photoproduct,
551 phenanthrenequinone. Environ. Toxicol. Chem. 16, 892-899.
- 552 Meckenstock, R.U., Morasch, B., Griebler, C., Richnow, H., 2004. Stable isotope fractionation
553 analysis as a tool to monitor biodegradation in contaminated aquifers. J. Contam.
554 Hydrol. 75, 215-255.
- 555 Nadal, M., Schuhmacher, M., Domingo, J.L., 2004. Levels of PAHs in soil and vegetation
556 samples from Tarragona County, Spain. Environ. Pollut. 132, 1-11.
- 557 Nadal, M., Schuhmacher, M., Domingo, J.L., 2011. Long-term environmental monitoring of
558 persistent organic pollutants and metals in a chemical/petrochemical area: Human health
559 risks. Environ. Pollut. 159, 1769-1777.
- 560 Nadal, M., Wargent, J.J., Jones, K.C., Paul, N.D., Schumacher, M., Domingo, J.L., 2006.
561 Influence of UV-B radiation and temperature on photodegradation of PAHs: Preliminary
562 results. J. Atmos. Chem. 55, 241-252.
- 563 Rivas, F.J., Beltran, F.J., Acedo, B., 2000. Chemical and photochemical degradation of
564 acenaphthylene. Intermediate identification. J. Hazard. Mater. B75, 89-98.
- 565 Roig, N., Sierra, J., Rovira, J., Schuhmacher, M., Domingo, J.L., Nadal, M., 2013. In vitro tests
566 to assess toxic effects of airborne PM₁₀ samples. Correlation with metals and chlorinated
567 dioxins and furans. Sci. Total Environ. 443, 791-797.
- 568 Salizzato, M., Rigioni, M., Pavoni, B., Volpi Ghirardini, A., Ghetti, P.F., 1997. Separation and
569 quantification of organic micropollutants (PAH, PCB) in sediments. Toxicity of extracts
570 towards *Vibrio fischeri*. Toxicol. Environ. Chem. 60, 183-200.
- 571 Shemer, H., Linden, K.G., 2007. Aqueous photodegradation and toxicity of the polycyclic
572 aromatic hydrocarbons fluorene, dibenzofuran, and dibenzothiophene. Water Res. 41,
573 853-861.
- 574 Singh, P., Mondal, K., Sharma, A., 2013. Reusable electrospun mesoporous ZnO nanofiber mats
575 for photocatalytic degradation of polycyclic aromatic hydrocarbon dyes in wastewater. J.
576 Colloid Interface Sci. 394, 208-215.
- 577 Wang, C., Wang, X., Gong, P., Yao, T., 2014. Polycyclic aromatic hydrocarbons in surface soil
578 across the Tibetan Plateau: Spatial distribution, source and air-soil exchange. Environ.
579 Pollut. 184, 138-144.

- 580 Wang, Y., Luo, C., Wang, S., Liu, J., Pan, S., Li, J., Ming, L., Zhang, G., Li, X., 2015. Assessment
581 of the Air–Soil Partitioning of Polycyclic Aromatic Hydrocarbons in a Paddy Field Using
582 a Modified Fugacity Sampler. *Environ. Sci. Technol.* 49, 284–291.
- 583 Xia, X., Li, G., Yang, Z., Chen, Y., Huang, G.H., 2009. Effects of fulvic acid concentration and
584 origin on photodegradation of polycyclic aromatic hydrocarbons in aqueous solution:
585 Importance of active oxygen. *Environ. Pollut.* 157, 1352-1359.
- 586 Xiaozhen, F., Boa, L., Aijun, G., 2005. Dynamics of solar light photodegradation behavior of
587 atrazine on soil surface. *J. Hazard. Mater.* B117, 75-79.
- 588 Zhang, L., Li, P., Gong, Z., Li, X., 2008. Photocatalytic degradation of polycyclic aromatic
589 hydrocarbons on soil surfaces using TiO₂ under UV light. *J. Hazard. Mater.* 158, 478-
590 484.
- 591 Zhang, L., Li, P., Gong, Z., Oni, A., 2006. Photochemical behavior of benzo[a]pyrene on soil
592 surfaces under UV light irradiation. *J. Environ. Sci.* 18, 1226-1232.
- 593 Zhang, L., Xua, C., Chena, Z., Li, X., Li, P., 2010. Photodegradation of pyrene on soil surfaces
594 under UV light irradiation. *J. Hazard. Mater.* 173, 168-172.
- 595 Zhang, X., Wu, Y., Hu, S., Lu, C., Yao, H., 2014. Responses of kinetics and capacity of
596 phenanthrene sorption on sediments to soil organic matter releasing. *Environ. Sci. Pollut.*
597 *Res.* 21, 8271–8283.
- 598 Zhao, X., Quan, X., Zhao, Y., Zhao, H., Chen, S., Chen, J., 2004. Photocatalytic remediation of
599 γ -HCH contaminated soil induced by α -Fe₂O₃ and TiO₂. *J. Environ. Sci.* 16, 938-941.

600

Arenosol soil

Regosol soil



◆ Irradiated samples -□- Dark controls

Fig. 1. Concentration of various PAHs in irradiated and dark control soil samples.

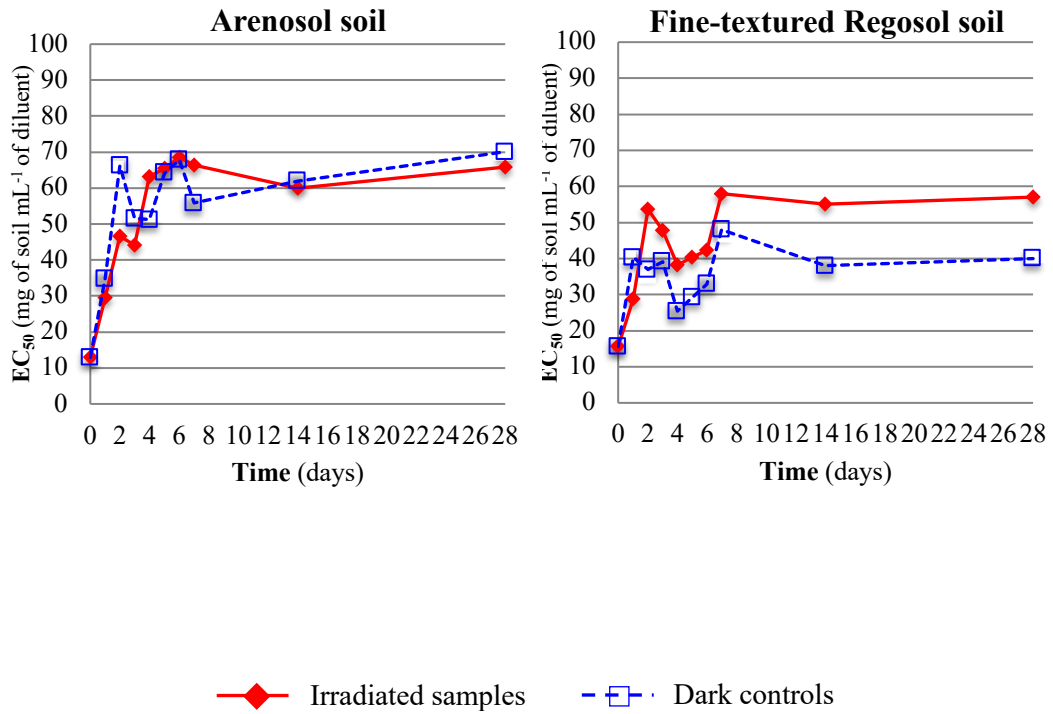


Fig. 2. Ecotoxicity of Arenosol and Regosol soil samples spiked with 16 PAHs.

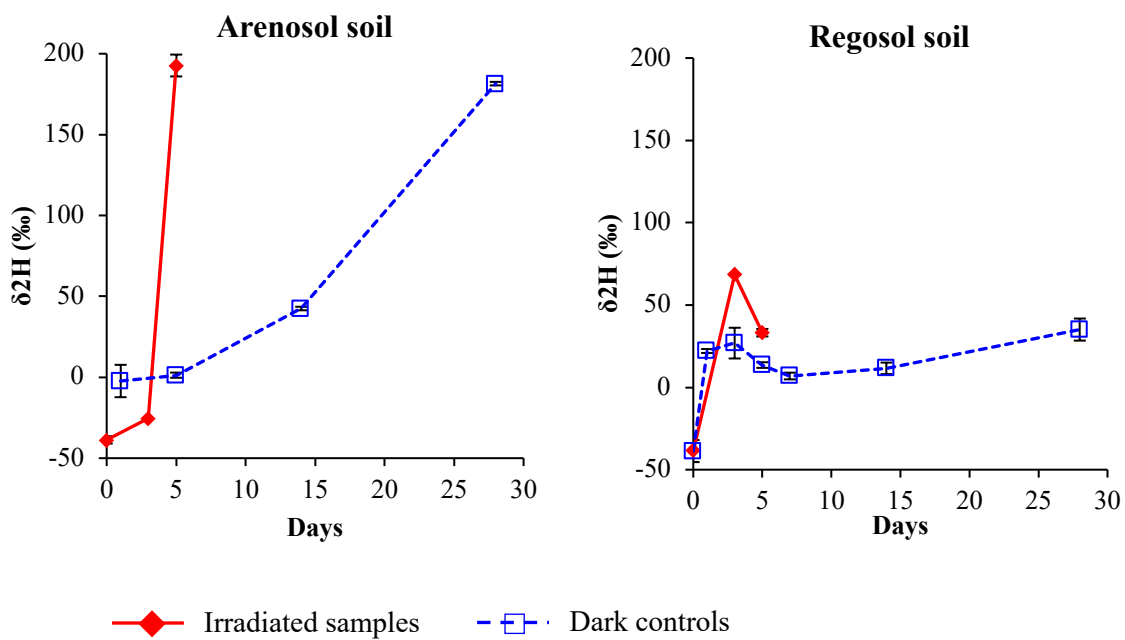


Fig. 3. Hydrogen isotopic composition of benzo(*a*)pyrene in Arenosol and Regosol soils in irradiated and dark control experiments.

Table 1

Physico-chemical properties of the selected Mediterranean soils.

	Arenosol soil	Regosol soil
pH	5.8	8.0
Electrical conductivity at 25 °C (dS m ⁻¹) ^a	0.06	0.13
Organic C (%) ^b	0.71	1.70
Total Kjeldahl N (%)	0.07	0.18
C/N	10.1	9.44
CaCO ₃ (%)	0.10	23.20
Texture: sand/silt/clay (%) ^c	74.1/14.0/11.9	43.4/22.3/34.3
Cation exchange capacity (meq 100 g ⁻¹) ^d	12.60	18.23
Exchangeable calcium (mg CaO kg ⁻¹) ^d	4.80	12.55
TiO ₂ (mg kg ⁻¹)	429	41.3
MnO ₂ (mg kg ⁻¹)	573	648
Al ₂ O ₃ (mg kg ⁻¹)	3008	6070
Fe ₂ O ₃ (mg kg ⁻¹)	6686	13492

Analytical methods: ^aAqueous extracts 1:2.5; ^bOxidizable C by Walkley-Black method; ^cRobinson Pipette method; ^d1 N ammonium acetate extracts.

Table 2

Statistical significance (p) of the regression associated to the photodegradation of PAHs.

Compound	Arenosol soil		Regosol soil	
	regression	p	regression	p
Naphthalene	exponential	0.277	exponential	0.955
Acenaphthylene	exponential	0.571	exponential	0.023
Acenaphthene	exponential	0.005	exponential	<0.0001
Fluorene	exponential	0.006	exponential	<0.0001
Phenanthrene	exponential	<0.0001	exponential	<0.0001
Anthracene	exponential	<0.0001	exponential	<0.0001
Fluoranthene	exponential	0.548	exponential	0.152
Pyrene	exponential	0.06	linear	0.134
Benzo(a)anthracene + chrysene	exponential	0.137	linear	0.095
Benzo(b+k)fluoranthene	exponential	0.039	linear	0.454
Benzo(a)pyrene	exponential	0.017	exponential	0.114
Benzo(ghi)perylene	exponential	0.409	exponential	0.120
Dibenzo(a,h)anthracene	exponential	0.058	exponential	0.131
Indeno(123-cd)pyrene	linear	0.289	exponential	0.004

In bold, statistically significant regression.

Table 3

Photodegradation rates (%) of the 16 PAHs under study in Arenosol and Regosol soils.

	Arenosol soil	Regosol soil
Naphthalene	0	0
Acenaphthylene	0	0
Acenaphthene	1.5	2
Fluorene	3	9.5
Phenanthrene	11.2	33.2
Anthracene	19.7	39.8
Fluoranthene	0	12.5
Pyrene	0	17.1
Benzo(<i>a</i>)anthracene + chrysene	0	30
Benzo(<i>b+k</i>)fluoranthene	0	30
Benzo(<i>a</i>)pyrene	23	4.9*
Benzo(<i>ghi</i>)perylene	3.6	24.6
Dibenzo(<i>a,h</i>)anthracene	2	28.3
Indeno(<i>123-cd</i>)pyrene	11.7	68.9

*completely degraded after 7 days of light exposure.